Subject: **Final Report**
NASA Grant #: **NAG5-10113**
Title: **An XMM Investigation of Non-Thermal Phenomena in the Winds of Early-Type Stars**
US PI: **Dr. Wayne L. Waldron**
Grant Period: **12/15/00 - 03/14/02**
Report Date: **3/26/02**

1. Assigned Tasks for Dr. Waldron

This report describes the work accomplished by Co-Investigator Dr. Wayne L. Waldron (L-3 Communications Analytics Corporation) on the analysis of an XMM-Newton observation of the O-star, 9 Sgr (O4V). Although time was awarded for a second target, HD168112, an O5III star, this target has not been observed due to scheduling issues.

Based on the limited award amount granted to Dr. Waldron, the Principle Investigator, Dr. Gregor Rauw (Institut d'Astrophysique, Universite de Liege, Liege, Belgium), assigned the following tasks to be carried out by Dr. Waldron in the analysis of the XMM observation of 9 Sgr:

1). generate best-fit stellar wind absorption models for the three EPIC spectra, EPIC-PN, EPIC-MOS1, and EPIC-MOS2;
2). determine if these fits are consistent with a previous ASCA SIS spectrum, and;
3). Assist the PI in the writing of papers to be presented at an ESTEC Symposium and a refereed article.

Section 2 provides a brief summary of this work, and additional details are discussed in the attached ESTEC Symposium paper (in press). In addition, a refereed journal article is in preparation entitled "A Multi-Wavelength Investigation of the Non-Thermal Radio Emitting O-Star 9 Sgr", G. Rauw, R. Blomme, W. L. Waldron, M. F. Corcoran, J. M. Pittard, A. M. T. Pollock, M. C. Runacres, H. Sana, I. R. Stevens, and S. Van Loo.

2. Summary of Analysis

The X-ray emission from early-type stars is believed to arise from a stellar wind distribution of shocks. Hence, X-ray analyses of these stars must include the effects of stellar wind X-ray absorption, which, in general dominates the ISM absorption. Although the absorption cross sections for the wind and ISM are essentially identical above 1 keV, there is substantial differences below 1 keV as shown in Figure 1. Typically, if one only uses ISM cross sections to obtain fits to X-ray spectra, the fits usually indicate a model deficiency at energies below 1 keV which is attributed to the large increase in ISM cross sections at these energies. This deficiency can be eliminated by using stellar wind absorption models with a fixed ISM component. Since all early-type stars have substantial X-ray emission below 1 keV, the inclusion of wind absorption has proven to be a critical component in fitting X-ray spectra at low energies, verifying that these X-rays are indeed arising from within the stellar wind.

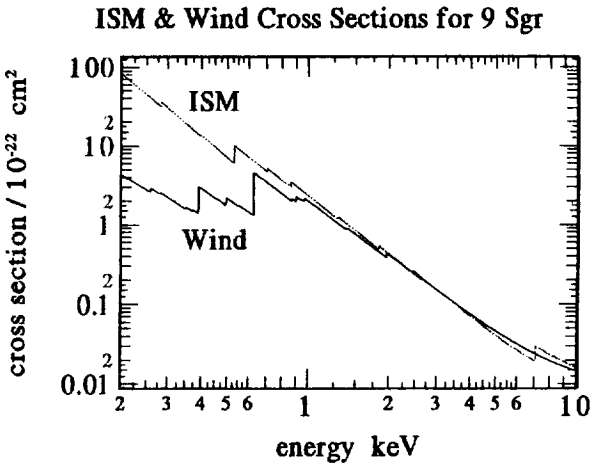

Figure 1 Comparison of the energy dependent ISM and wind cross sections over the effective energy range of the EPIC.

Using stellar wind absorption models and MEKAL emissivities, best-fit models were obtained for the XMM EPIC-PN, EPIC-MOS1, and EPIC-MOS2 spectra. A minimum of three components were

required in order to obtain good fits to the data. The best fit parameters are listed in Table 1; T_X (X-ray temperature), EM_X (X-ray emission measure), N_W (stellar wind column density), and the total observed flux from all three components for each instrument. For the first and second components the errors on the derived parameters are ~ 10% for T_X and ~ 30% for both EM_X and N_W. For the third component, the value of T_X and N_W are not well constrained where any $T_X > 20$ MK is acceptable, and there is essentially no constraint on N_W (e.g., values from 0-100x10^{21} cm^{-2} are acceptable). The actual best fit for this component appears to always occur at the highest T_X and N_W, and for all models N_W is set equal to the maximum wind column density and T_X is set equal to 100 MK. All models use an ISM column density fixed at the observed E(B-V) determined value of 2.2x$10^{21}$$cm^{-2}$. In addition, a best-fit model of the ASCA SIS0 spectrum is also included.

The models fits are shown in Figure 2 for the EPIC-PN and EPIC-MOS2 which show the overall fit and contributions from each component. The fits were found to be very good with reduced χ^2 of 1.1 (PN), 1.7 (MOS1), and 1.3 (MOS2). The total predicted observed flux (0.5-10 keV) from the EPIC instruments are found to be consistent to within ~ 10%. In addition, the XMM flux is within ~ 25% of the observed flux determined from ASCA data (observed ~ 4 years earlier) which is in agreement with other long time scale measurements for other O-stars, suggesting that the observed X-ray flux is relatively stable. The presence of a high T_X third component represents the first strong evidence that O-stars may possess thermal X-ray emission at temperatures > 20 MK. The thermal nature of this component is supported by the presence of He-like Fe XXV (~ 6.6 keV) emission lines which are only visible in the higher S/N EPIC-PN spectrum. Additional higher S/N observations will be needed to verify these results.

Table 1. Best Fit Parameters for Stellar Wind Absorption Models

instrument	1st component			2nd component			3rd component			obs Flux
	T_X	EM_X	N_W	T_X	EM_X	N_W	T_X	EM_X	N_W	erg cm^{-2} s^{-1}
EPIC-PN	3.00	31.1	2.62	7.14	13.6	15.3	100.0	0.91	44.7	1.90x10^{-12}
EPIC-MOS1	2.98	33.2	3.41	8.20	6.02	10.6	100.0	1.02	44.7	1.72x10^{-12}
EPIC-MOS2	2.84	30.5	2.77	7.94	6.56	8.57	100.0	1.02	44.7	1.79x10^{-12}
ASCA SIS0	3.30	37.50	5.18	12.9	5.90	9.08	100.0	3.23	44.7	2.13x10^{-12}

NOTE- T_X is in units of MK; EM_X is in units of 10^{55} cm^{-3}; N_W is in units of 10^{21} cm^{-2}.

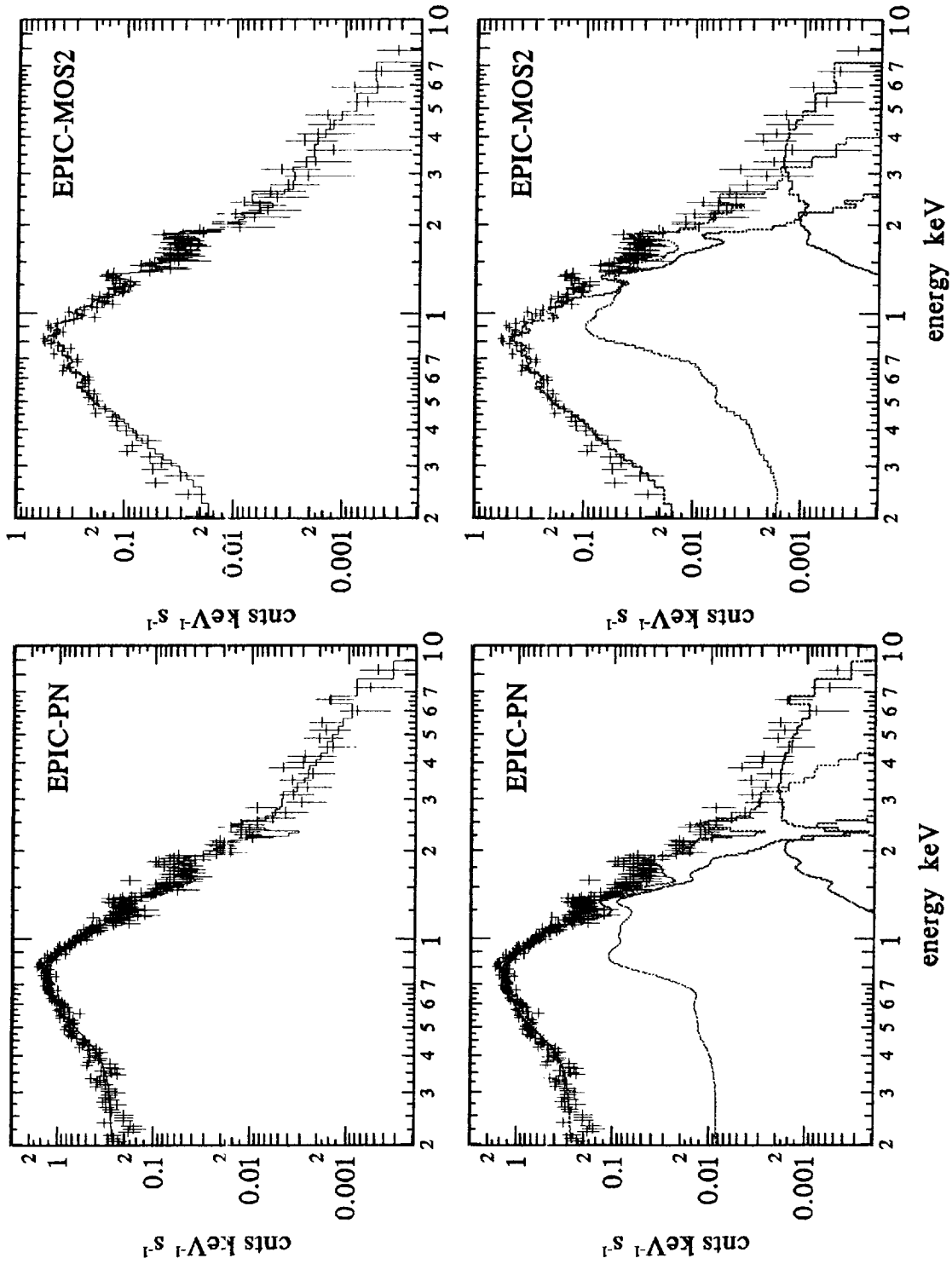

Figure 2 Best fit models for the EPIC-PN and EPIC-MOS2 spectra of 9 Sgr. The top panels show the total fits and the bottom panels show the individual contributions from the three components. The spectra have been rebind such that there are at least 10 counts per bin.

AN XMM-NEWTON STUDY OF 9 SGR AND THE LAGOON NEBULA

G. Rauw[1], R. Blomme[2], W.L. Waldron[3], Y. Nazé[1]*, T.J. Harries[4], J.M. Chapman[5], M.F. Corcoran[6], A. Detal[1], E. Gosset[1], J.M. Pittard[7], A.M.T. Pollock[8], M.C. Runacres[2], H. Sana[1]*, I.R. Stevens[9], S. Van Loo[2], and J.-M. Vreux[1]**

[1]Institut d'Astrophysique, Université de Liège, Allée du 6 Août, Bât B5c, B-4000 Liège (Sart Tilman), Belgium
[2]Royal Observatory Belgium, Avenue Circulaire 3, B-1180 Brussels, Belgium
[3]Emergent Technology Services, Space Sciences Sector, 1801 McCormick Drive, Suite 170, Largo, MD 20774, USA
[4]School of Physics, University of Exeter, Stocker Road, Exeter EX4 4QL, UK
[5]Anglo-Australian Observatory, P.O. Box 296 and Australia Telescope National Facility, P.O. Box 76, Epping, NSW 2121, Australia
[6]USRA/HEASARC Goddard Space Flight Center, Greenbelt, MD 20771, USA
[7]Department of Physics & Astronomy, University of Leeds, Leeds LS2 9JT, UK
[8]Computer & Scientific Co. Ltd., 230 Graham Road, Sheffield S10 3GS, UK
[9]School of Physics & Astronomy, University of Birmingham, Edgbaston Birmingham B15 2TT, UK

ABSTRACT

We report preliminary results of an XMM-Newton observation of the O4 V star 9 Sgr (= HD 164794). 9 Sgr is one of a few single OB stars that display a non-thermal radio emission attributed to synchrotron emission by relativistic electrons. Inverse Compton scattering of photospheric UV photons by these relativistic electrons is a priori expected to generate a non-thermal power-law tail in the X-ray spectrum. Our EPIC and RGS spectra of 9 Sgr suggest a more complex situation than expected from this 'simple' theoretical picture.
Furthermore, soft-band EPIC images of the region around 9 Sgr reveal a number of point sources inside the Lagoon Nebula (M 8). Most of these sources have optical counterparts inside the very young open cluster NGC 6530 and several X-ray sources are associated with low and intermediate mass pre-main sequence stars. Finally, we also detect (probably) diffuse X-ray emission from the Hourglass Region that might reveal a hot bubble blown by the stellar wind of Herschel 36, the ionizing star of the HG region.

Key words: Radiation mechanisms: non-thermal – Stars: early-type – Stars: individual: 9 Sgr – Stars: pre-main sequence – X-rays: stars

1. INTRODUCTION

Single O-stars display thermal X-ray emission that is usually attributed to hydrodynamic shocks produced by instabilities in their stellar winds (see e.g. Feldmeier et al. 1997). These shocks are also believed to be efficient sites for the acceleration of relativistic electrons through the first order Fermi process (e.g. Chen & White 1994). Indeed, the existence of a small population of relativistic electrons is revealed by the non-thermal synchrotron emission that is observed at radio wavelengths in a particular subset of O-stars (e.g. Bieging et al. 1989).
Given the enormous supply of photospheric UV photons in the winds of OB stars, inverse Compton scattering is expected to become the major energy loss mechanism for relativistic electrons and substantial levels of non-thermal X-ray and low energy γ-rays should be generated, resulting approximately in a power-law spectrum from keV to MeV energies (Chen & White 1991).

We selected the probably single O4 V((f)) star 9 Sgr (= HD 164794) to investigate this phenomenon. 9 Sgr is known to display a variable non-thermal radio emission. The star is located in the Lagoon Nebula (M 8) and has been extensively studied at UV and visible wavelengths.

2 OBSERVATIONS AND DATA REDUCTION

We obtained a 20 ksec AO1 observation of 9 Sgr with XMM-Newton (JD 2451976.978 – 2451977.239). We used the SAS version 5.1 to reduce the raw EPIC data while the RGS observations were processed with version 5.0.1 of the SAS software. The EPIC data are significantly affected by single mirror reflection photons from the low-mass X-ray binary Sgr X-3 (GX 9 +1)located at $\sim 1^\circ$ from the center of the field of view. The spectrum of the straylight features near 9 Sgr can be fitted with a heavily absorbed blackbody model with $N_H = (3.1 \pm 0.3) \times 10^{22}$ cm^{-2} and kT = 1.04 ± 0.05 keV. The straylight photons are therefore rather hard and there is nearly no contamination of the EPIC data in the soft energy range E $\in]0.2, 1.5[$ keV.

We accumulated the EPIC spectra of 9 Sgr over a radius of 45″ excluding the intersection with a small circular region centered on a faint point-like source (XMMU J180350.5-242110). The background spectra for the different data sets were obtained over rectangular areas selected to avoid the straylight features. We have also tested a different background subtraction technique using the back-

* Research Fellow FNRS (Belgium)
** Research Associate FNRS (Belgium)

Proc. Symposium *'New Visions of the X-ray Universe in the XMM-Newton and Chandra Era'* 26–30 November 2001, ESTEC, The Netherlands
ESA SP-488, August 2002 eds. F. Jansen & TBD

ground files provided by the XMM-SOC. The background subtracted spectra of 9 Sgr obtained in either way do not show any significant difference.

3. X-RAY EMISSION FROM 9 SGR

3.1. THE EPIC SPECTRUM

The background corrected spectra of 9 Sgr were analyzed using the XSPEC software (version 11.00). We considered a couple of rather simple spectral models. In these fits, we always fixed the interstellar H I column density at 2.2×10^{21} cm^{-2} (Shull & van Steenberg 1985).
To start, we tested absorbed two-temperature `mekal` and absorbed 1-T `mekal` + `power-law` models (see Fig. 1). In our first attempt, the column densities derived from the spectral fits refer to the circumstellar (i.e. wind) material considered here to be completely neutral. Two problems emerge from this simple analysis:

- The best fitting parameters yield a column density for at least one model component that is extremely small.
- The 1-T + `power-law` fits are usually better than the 2-T fits. However, these fits yield systematically large photon indices ($\alpha \geq 3.8$), much larger than the ~ 1.5 value expected from the Chen & White (1991) model. The reason for this steep power-law is that the 1-T thermal component fails to account for the observed flux at energies below 0.5 keV and the power-law has to provide the flux to compensate for this. Such a steep power-law can however be ruled out by the RGS data. In fact, the RGS spectra display strong line emission (see Fig. 2) and the X-ray emission of 9 Sgr must therefore be thermal at lower energies

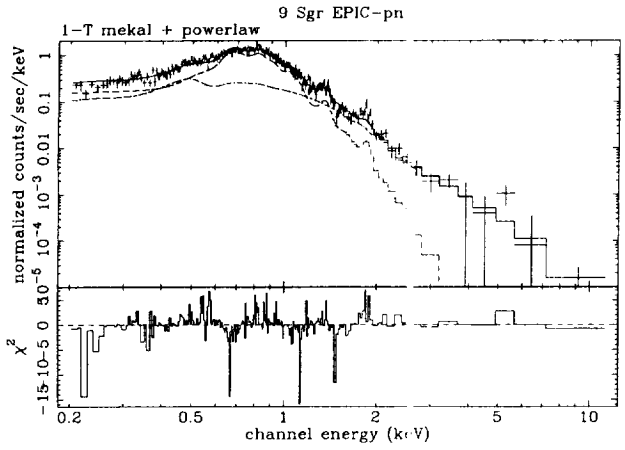

Figure 1. EPIC-pn spectrum of 9 Sgr together with the best-fitting 1-T `mekal` + `power-law` *model.*

To solve the first problem, we fitted the EPIC spectra with wind absorption models (see Waldron et al. 1998). These models are computed using stellar and wind parameters appropriate for 9 Sgr and account therefore for the ionization of the stellar wind. The EPIC spectra of 9 Sgr can be fitted with a 3-T model although the highest temperature component ($kT_3 \in [6, 8.6]$ keV) is not well constrained by our data.

3.2. THE RGS SPECTRUM

The RGS spectrum of 9 Sgr is reminiscent of that of ζ Pup (Kahn et al. 2001). The most prominent features are the He-like triplets of Ne IX and O VII, the Lyα lines of Ne X, O VIII and N VII as well as several L-shell lines of Fe XVII (see Fig. 2).

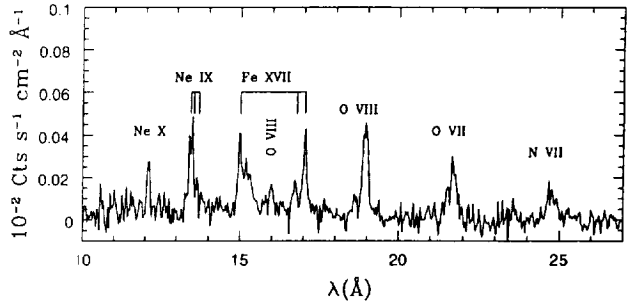

Figure 2. First order RGS 1 + 2 spectrum of 9 Sgr. The strongest emission lines are identified.

In the presence of the strong ultraviolet radiation field of an O-star, the ratio $\mathcal{R} = f/i$ of He-like triplets is determined by the intensity of the UV radiation (e.g. Waldron & Cassinelli 2001). In the case of 9 Sgr, the observed $\mathcal{R}$ ratio of the Ne IX line (~ 0.4) suggests that this line forms rather far out in the wind.
Our data also reveal a systematic blue-shift of the line centroids in all strong lines. Such a blue-shift is expected for lines formed in an accelerating stellar wind since radiation from the approaching side of the wind should be less attenuated by continuum opacity than that from the receding part (Owocki & Cohen 2001).

3.3. SIMULTANEOUS VLA RADIO OBSERVATIONS

We observed 9 Sgr with the NRAO VLA (Very Large Array) simultaneously (JD = 2451977.012–.037) with the XMM-Newton observations. Data were collected at 3.6, 6 and 20 cm. The data reduction was done using the Astronomical Image Processing System (AIPS), developed by the NRAO. Due to the presence of other bright sources in the field, the main source of error in the fluxes is the uncertainty in the background subtraction.

The resulting spectral indices ($\alpha_{3.6-6} = -1.0$) clearly indicate the non-thermal character of the radio emission

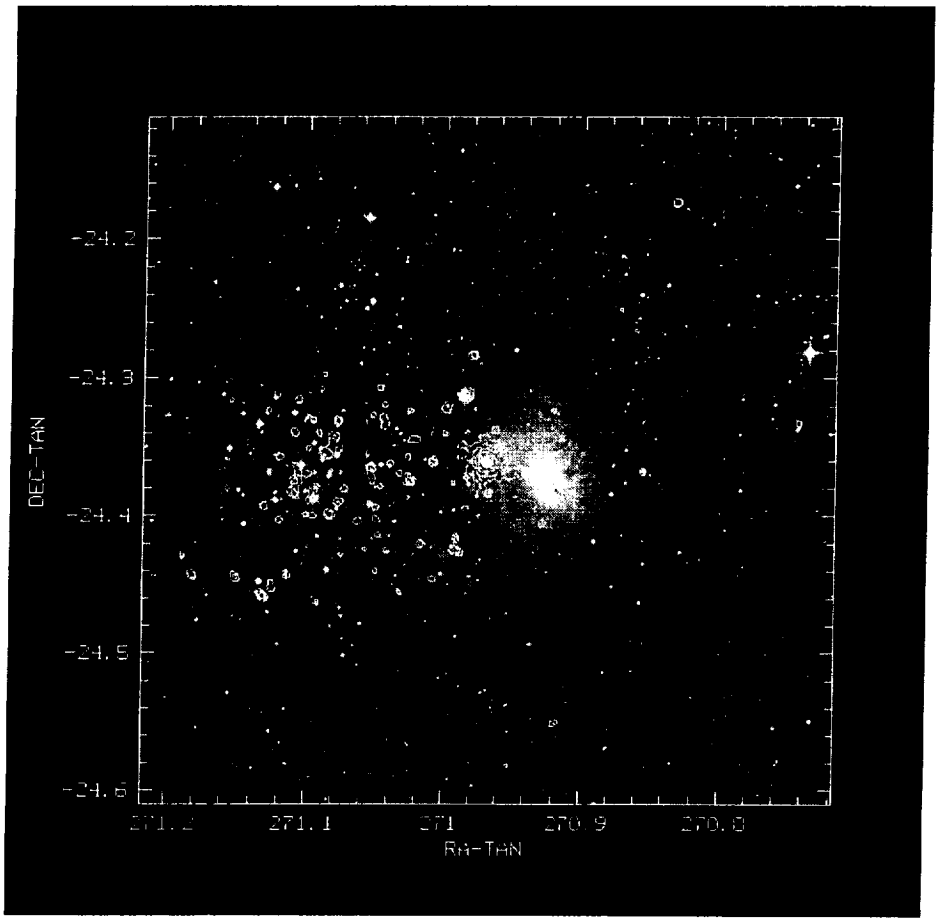

Figure 3. DSS optical image centered on 9 Sgr. X-ray contours (corresponding to the combined MOS1 + MOS2 data) are overlaid on this image. The different contours correspond to 2, 4, 8, 16 and 64 counts over the 0.2 – 1.5 keV range in the X-ray image.

from 9 Sgr and the fluxes are on the high side of the range covered by values in the literature (Bieging et al. 1989).

4. X-ray sources inside the Lagoon Nebula

The combined MOS1 + MOS2 soft (0.2 – 1.5 keV) X-ray image around 9 Sgr reveals 71 point-like sources down to an observed flux of 6×10^{-15} erg cm^{-2} s^{-1} over this energy range. Most of the fainter sources are located in the region of the very young open cluster NGC 6530 which is embedded in the Lagoon Nebula (M 8). One rather bright and apparently diffuse source (to the south-west of 9 Sgr) is associated with the Hourglass Region.

43 X-ray sources out of these 71 have a single optical counterpart (within a radius of 12″) from the catalogue of Sung et al. (2000). The X-ray brightest objects in this category are HD 164816 (O9.5 III-IV) and SCB 731. The light curve of SCB 731 reveals a strong X-ray flare towards the end of our observation (see Fig. 4).

We have plotted the X-ray sources with a single optical counterpart in a $(B-V, V)$ colour-magnitude diagram. Apart from a group of rather bright ($V \leq 12$) stars that are probably early-type OB stars, we find a group of objects lying to the right of the ZAMS (by about 0.5 in $B-V$). Three of these objects display Hα emission and are classified as pre-main sequence (PMS) stars (Sung et al. 2000).

There are 32 X-ray sources that have optical counterparts fainter than 12th magnitude and we suggest that these are good candidates for weak-line T Tauri stars. The fact that only a few X-ray selected PMS candidates display an Hα emission is in agreement with the theoretical picture that the X-ray bright PMS stars are more evolved objects without a prominent circumstellar disk.

Our EPIC data also unveil an extended X-ray emission from the Hourglass Region in M 8. This emission is probably due to the contributions of the young stellar object Herschel 36, the UC HII region G 5.97 −1.17 and possibly a diffuse emission from a hot bubble created by the wind of Herschel 36.

5. Conclusions

Our XMM observations indicate that there exists a hard X-ray component in the spectrum of 9 Sgr. The exact na-

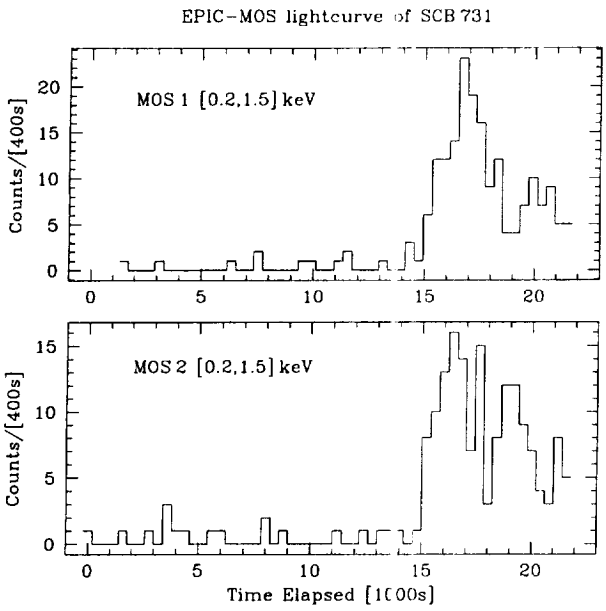

Figure 4. EPIC-MOS light curves of the X-ray source XMMU J180435.5-242729 associated with SCB 731. We have also extracted the light curve of a nearby background region. The latter does not show any variability.

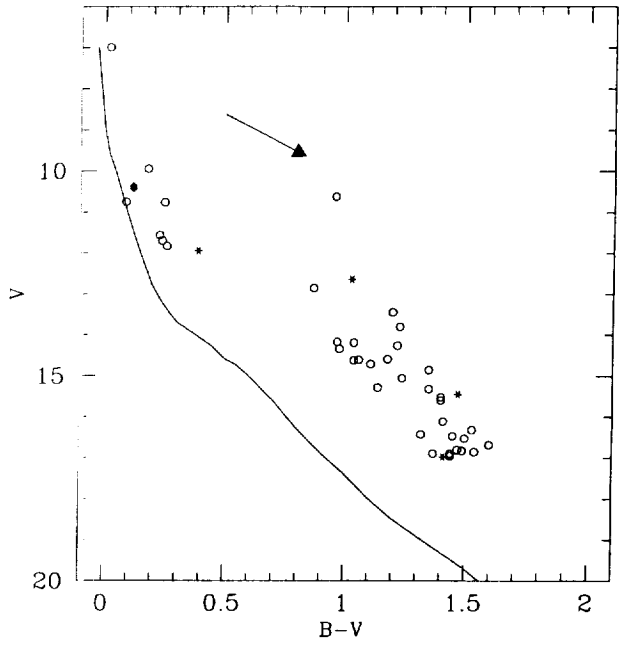

Figure 5. Colour-magnitude diagram of the X-ray sources in the field of view of the very young open cluster NGC 6530. The reddening vector with $R = 3.1$ is indicated and the solid line shows the ZAMS relation with a distance modulus $DM = 11.25$ and reddened with $E(B-V) = 0.30$. Open symbols stand for stars from Sung et al. (2000) without Hα emission, asterisks stand for pre-main sequence stars or PMS candidates from Sung et al. and the filled diamonds indicate two stars classified as Be stars by van den Ancker et al. (1997).

ture of this component is however not clear and our data seem at odds with the predictions of the model of Chen & White (1991). Though radio observations clearly reveal the presence of relativistic electrons, it remains to be seen whether inverse Compton scattering can account for the properties of the observed hard X-rays. Quantitative theoretical models as well as more XMM-Newton data on non-thermal radio emitting O-stars are badly needed.
The RGS spectrum of 9 Sgr displays strong line emission reminiscent of the RGS spectra of other early-type O-stars such as ζ Pup. The properties of these lines suggest that the emitting plasma is distributed throughout the accelerating stellar wind.

Soft-band EPIC images of the Lagoon Nebula reveal many point sources. Most of these sources have optical counterparts inside the very young open cluster NGC 6530 and a few are associated with known low- and intermediate mass PMS stars. From their location in a colour-magnitude diagram and from the flaring behaviour of the brightest source, we suggest that many of our new sources correspond to weak-line T Tauri stars.

A more detailed analysis of the XMM observation of 9 Sgr and the Lagoon Nebula will be presented in a forthcoming paper.

Acknowledgements

We are grateful to Barry Clark for kindly scheduling the VLA radio observation simultaneously with the XMM observation. The Liège team acknowledges support from the Fonds National de la Recherche Scientifique (Belgium) and through the PRODEX XMM-OM and Integral Projects. This research is also supported in part by contract P4/05 "Pôle d'Attraction Interuniversitaire" (SSTC-Belgium). WLW was supported in part by NASA contract # NAG 5-10113.

References

Bieging, J.H., Abbott, D.C., & Churchwell, E.B. 1989, ApJ, 340, 518
Chen, W., & White, R.L. 1991, ApJ, 366, 512
Chen, W., & White, R.L. 1994, Ap&SS, 221, 259
Feldmeier, A., Puls, J., & Pauldrach, A.W.A. 1997, A&A, 322, 878
Kahn, S.M., Leutenegger, M.A., Cottam, et al. 2001, A&A, 365, L312
Owocki, S.P., & Cohen, D.H. 2001, ApJ, 559, 1108
Shull, J.M , & van Steenberg, M.E. 1985, ApJ, 294, 599
Sung, H., Chun, M.-Y., & Bessell, M.S. 2000, AJ, 120, 333
van den Ancker, M.E., Thé, P.S., Feinstein, A., et al. 1997, A&AS, 123, 63
Waldron, W.L., Corcoran, M.F., Drake, S.A., & Smale, A.P., 1998, ApJS, 118, 217
Waldron, W.L., & Cassinelli, J.P., 2001, ApJ, 548, L45